GEOPHYSICS, VOL. 71, NO. 4 (JULY-AUGUST 2006); P. B101–B109, 9 FIGS., 1 TABLE.
10.1190/1.2210307

Case History

High-resolution geophysical characterization of shallow-water wetlands

Nasser Mansoor[1], Lee Slater[1], Francisco Artigas[2], and Esben Auken[3]

ABSTRACT

We describe a procedure for rapid characterization of shallow-water, contaminated wetlands. Terrain-conductivity (TC), vertical-magnetic-gradiometry, and surface-water-chemistry data were obtained from a shallow-draft paddle-boat operable in as little as 0.3 m of water. Measurements were taken every 2 s, with data-acquisition rates exceeding 10 km of line ($>$12 000 data points) per 8-hr field day.

We applied this procedure to an urban wetland that is affected by point and nonpoint sources of pollution. We used a one-dimensional, laterally constrained inversion algorithm to invert the apparent-conductivity data set obtained from the TC survey and to create a pseudo-2D image of sediment conductivity. The continuously recorded surface-water depth and conductivity values were input as a priori information in the inversion. We used soil chemistry determined for 28 sediment samples collected from the site, as well as lithologic logs from across the wetland, to constrain interpretation of the geophysical data. The inverted sediment conductivity describes a pattern of contamination probably attributable to leachates from adjacent landfills and/or to saltwater ingress from a partial tidal connection that is not obvious in the surface-water data. Magnetic-gradiometry values and the in-phase component of an EM31 response both reflect primarily the distribution of junk metal associated with a legacy of illegal dumping. Historic aerial photographs suggest that this distribution reflects land-use history and defines the maximum previous extent of an adjacent landfill and a pattern of dumping correlated with historic roadways.

INTRODUCTION

Once considered to be useless, disease-ridden environments, wetlands now are known to perform many ecological functions and to provide numerous societal benefits. Wetlands temporarily store water, reduce flooding, cycle nutrients, maintain characteristic plant communities, and provide diverse wildlife habitats (Smith et al., 1995; Uranowski et al., 2003).

Effective subsurface-investigation strategies are required for facilitating wetlands characterization, protection, and restoration. For example, in tidal wetlands the geometry of the freshwater-saltwater interface regulates ecosystem communities by determining the distribution of salinity. In wetlands fringing on urban areas, contamination resulting from leakages from containment structures and industrial facilities is a detriment to wetlands restoration. Direct sampling methods can be destructive to wetland vegetation and may provide only sparsely sampled data that give uncertain realizations of the spatial variability in physicochemical properties of wetland sediments. Furthermore, waterlogged wetland soils typically hinder foot or vehicular access. Where surface water exists, access to the wetland using a boat with sampling equipment often is difficult.

Geophysical methods provide noninvasive, spatially extensive proxy measurements of the physicochemical properties of the subsurface and are capable of delineating groundwater contamination (e.g., Greenhouse and Harris, 1983; McNeill, 1990; Kobr and Linhart, 1994; Woldt et al., 1998). Electromagnetic terrain-conductivity (TC) surveys are employed extensively in site characterization on land. Common applications for such surveys include evaluating groundwater quality (McNeill, 1980), mapping soil moisture content (Kachanoski et al., 1988; Sheets and Hendrickx, 1995), and delineating contaminant plumes from landfills (Greenhouse and Harris, 1983; Matias et al., 1994; Benson et al., 1997; Meju, 2000; Buselli and Lu, 2001). In saturated soils, terrain conductivity de-

Manuscript received by the Editor January 21, 2005; revised manuscript received December 23, 2005; published online July 28, 2006.
[1]Rutgers University, Department of Earth and Environmental Sciences, 101 Warren Street, Newark, New Jersey 07102. E-mail: nmansoor@pegasus.rutgers.edu; lslater@andromeda.rutgers.edu.
[2]Meadowlands Environment Research Institute (MERI), 1 DeKorte Park Plaza, Lyndhurst, New Jersey 07071. E-mail: francisco.artigas@njmeadowlands.gov
[3]University of Aarhus, Department of Earth Sciences, HydroGeophysics Group, Finlandsgade 8, DK-8200, Denmark. E-mail: esben.auken@geo.au.dk.

pends on the electrolytic conductivity of the pore fluid, on soil moisture content, and on soil lithology. Quantitative information about subsurface conductivity can be derived from inversion of apparent-conductivity data, using a priori information obtained from borehole and laboratory data. In shallow-water wetlands, we can measure the surface water's depth and conductivity at the same time that we record terrain conductivity, and in so doing, we can invert for the conductivity of the wetland sediments.

Magnetic methods are effective for mapping the distribution of ferromagnetic debris (primarily iron) and the location of buried drums and pipes in urban areas (Ravat, 1996; Furness, 2002). Measurement of the gradient of the magnetic field between two sensors (as opposed to the total-field magnitude) enhances the effects of near-surface objects relative to the effects of deeper structures. Roberts et al. (1990) used a magnetic survey to delineate the extent of an old landfill. Pozza et al. (2004) employed lake-based magnetic surveys in Hamilton Harbor, Canada and successfully mapped the extent of contamination in the harbor sediments.

Although geophysical methods are used extensively for noninvasive subsurface characterization, very few reported studies exist that describe implementation of geophysical technologies in shallow-water wetland environments. In this study, we used TC and magnetic-gradiometry surveys from shallow-water boats to devise and test an approach to wetlands investigations. We favor such noncontact geophysical techniques over direct-contact methods (e.g., over electrical imaging) because they can be deployed easily from a shallow-water boat, thereby allowing rapid data acquisition over a large area when they are interfaced with a differential GPS measurement for spatial location. Furthermore, we expect these noncontact techniques to provide two complementary pieces of information about industrial wetland characterization: (1) the spatial distribution of pore-water-conductivity values that reflect contamination sources fringing the wetland and (2) the spatial distribution in the wetland of junk metal associated with historic illegal dumping.

We demonstrate our wetland-characterization approach by reporting the results of an urban-wetland study aimed at (1) evaluating the extent of contamination attributable to landfills abutting our study site's marsh and to a relict tidal connection, and (2) determining the distribution and amount of metallic debris in the marsh sediments. We also assess the influence of the surface-water layer on EM31-measured apparent conductivity and thereby evaluate the ability of TC to map the conductivity of wetland sediments beneath the water layer.

STUDY SITE: KEARNY MARSH, HACKENSACK MEADOWLANDS

Our study site is Kearny Marsh, a freshwater wetland located in the New Jersey Meadowlands District, USA (Figure 1). The Meadowlands District covers an area of about 83 km^2 and is an ecologically complex system that is severely impacted by human activities — most notably by the practice of draining and infilling wetlands for landfills and development projects. By 1969, 51 locations of landfill operations, which accounted for more than 10 km^2, were identified in the district. Wetlands and water now cover only about 34 km^2 of the district.

Kearny Marsh, an approximately 1.3-km^2 freshwater wetland located at the southern end of the district, is, by area 55% shallow open water and 45% colonies of hydrophilic vegetation. Surface water in the marsh fluctuates seasonally and has an average depth of less than 0.75 m. Multiple point and nonpoint sources of pollution potentially impact the marsh. One pollution source is the approximately 0.45 km^2 Keegan Landfill, which abuts the marsh's southwestern corner (Figure 1). Keegan Landfill operated as an unlined landfill between the mid-1960s and the 1970s. Contaminated discharge to both groundwater and surface water is assumed to have occurred from the Keegan landfill (Langan Engineering and Environmental Services, 1999). Other potential sources of pollutants include the 1E Landfill to the northeast, the 15W Landfill to the south, a metal junkyard to the northwest, an aggregates-processing facility to the west, and the New Jersey Turnpike and other highways (Figure 1).

Kearny Marsh became a closed freshwater system (having no natural inlets or outlets) after installation of the 1970 extension of the New Jersey Turnpike, which separated the marsh from tidal flow of the Hackensack River on the east. Topography and survey data of groundwater levels indicate that the general direction of groundwater flow is to the east and southeast and from the Keegan Landfill into the marsh (Kocis, 1982). However, the topography of the 1E Landfill also is assumed to drive groundwater into the marsh (Figure 1). A hydrologic study conducted in 1982 suggests that the northeastern area of the marsh might still be affected by a tidal connection south of the 1E Landfill (Kocis, 1982) (Figure 1).

The marsh is underlain by peat and clay, both of which have traces of sand, silt, and gravel. The soil stratigraphy consists of peat and organic-rich silt (~2 m thick) underlying the fill and overlying a relatively thick sand layer (5 m thick, on av-

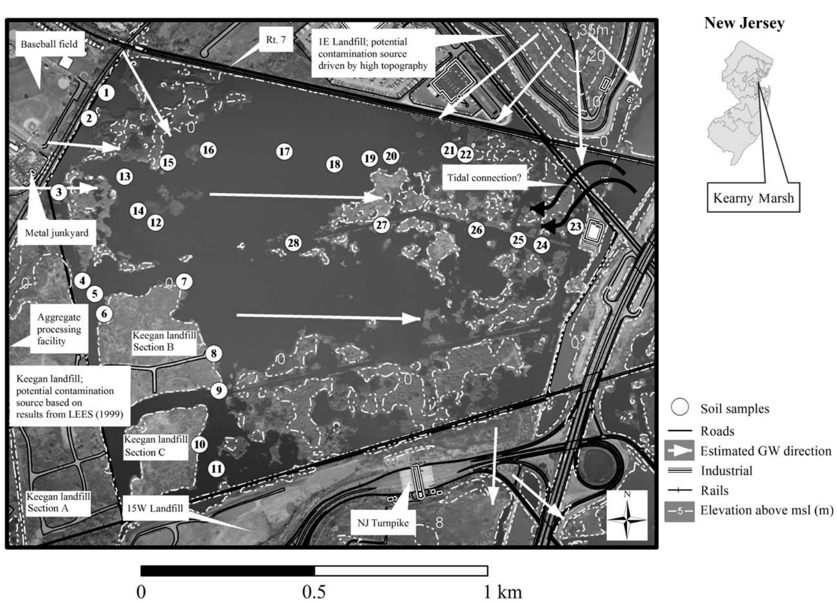

Figure 1. A site map delineating Kearny Marsh, a freshwater marsh in New Jersey, USA. The map shows landfills and other identified zones of potential contamination sources, locations of pore-water and sediment sample sites (circled numbers), land-use /characteristics, and ground-elevation contours (dashed-numbered lines). Hydrophilic vegetation (light gray shading of the 2002 aerial photos) colonizes 45% of the marsh, and surface water is the darker gray area. The inset shows the site location in New Jersey.

erage). The sand is underlain by a silt layer with an average thickness of 10 m. A thick gray to reddish brown varved clay deposit with silt lies beneath this sequence and has a maximum thickness of about 27 m. The varved clay is underlain by reddish-brown, poorly graded sandy gravel with traces of silt. Figure 2 summarizes the variation in subsurface stratigraphy as well as in surface-water depth, in the marsh.

GEOPHYSICAL DATA ACQUISITION IN SHALLOW-WATER WETLANDS

We used an all-plastic (excluding the steering mechanism) four-person paddleboat, typically used for recreation on small lakes and ponds, for rapid acquisition of our geophysical data in these shallow-water wetlands (Figure 3). The boat's shallow draft (approximately 0.3 m) is ideal for operation in such wetlands. The paddleboat was equipped with the following instrumentation: a high-precision Trimble® differential GPS unit (with a location accuracy of ±25 cm), a digital surface-water-quality probe (to record temperature, pH, electrical conductivity, salinity, total dissolved solids, dissolved oxygen, turbidity, and water depth), a digital magnetic gradiometer, and a digital terrain-conductivity meter (Figure 3 shows these last two instruments in the boat for illustration purposes only), and finally, a waterproof laptop computer. Instruments were time synchronized to within 1 s, and a time stamp was used to tie geophysical data to their corresponding locations recorded by GPS. All instruments were programmed to automatically record a measurement every 2 s during the survey. Geophysical data acquisition rates exceeded 10 km of line ($>$12,000 measurements) per 8-hr field day.

The EM31 terrain-conductivity meter was mounted to the paddleboat in vertical-dipole configuration, with a fixed orientation perpendicular to the survey direction at 45 ± 2 cm above the surface water (Figure 3). Prior to data collection, both components of the EM31 (quadrature and in-phase) instrument were calibrated at a nearby recreational park that lacked any objects that might interfere with the instrument. Because of the shallow water depth, the EM31 quadrature response was expected to reflect primarily the electrical conductivity of the sediments, as we discuss later.

A Scintrex Envi™ vertical gradiometer was employed with the magnetometer sensors placed in a custom-made all-PVC attachment 1.5 m off the back end of the boat. A field test determined that this distance would remove any interference from the metallic steering mechanism of the boat and on-board instrumentation (e.g., GPS, laptop). The test was performed analyzing the magnetometer response as a function of azimuth. Our field tests revealed that a distance of 1.5 m was required to eliminate artifacts resulting from orientation (i.e., the gradient and the total magnetic field reading were stable and showed no dependence on survey orientation). The base of the bottom sensor of the magnetometer was placed 1.3 ± 0.05 m above the surface water. The vertical separation between sensors was 0.5 m. At all times during data collection, a manually controlled mechanical device (rope attached to the sensor frame) was used to keep the magnetometer sensors pointing northward.

Surface-water parameters were also measured simultaneously with geophysical measurements, using a Hydrolab™ probe mounted to the front of the paddleboat (Figure 3). The measured parameters were surface-water electrical conductivity, temperature, pH, and water depth. The depth and the electrical conductivity were required to constrain inversion of the TC data set. All apparent-conductivity, gradiometry, and surface-water-chemistry data were recorded at 2-s intervals during the survey.

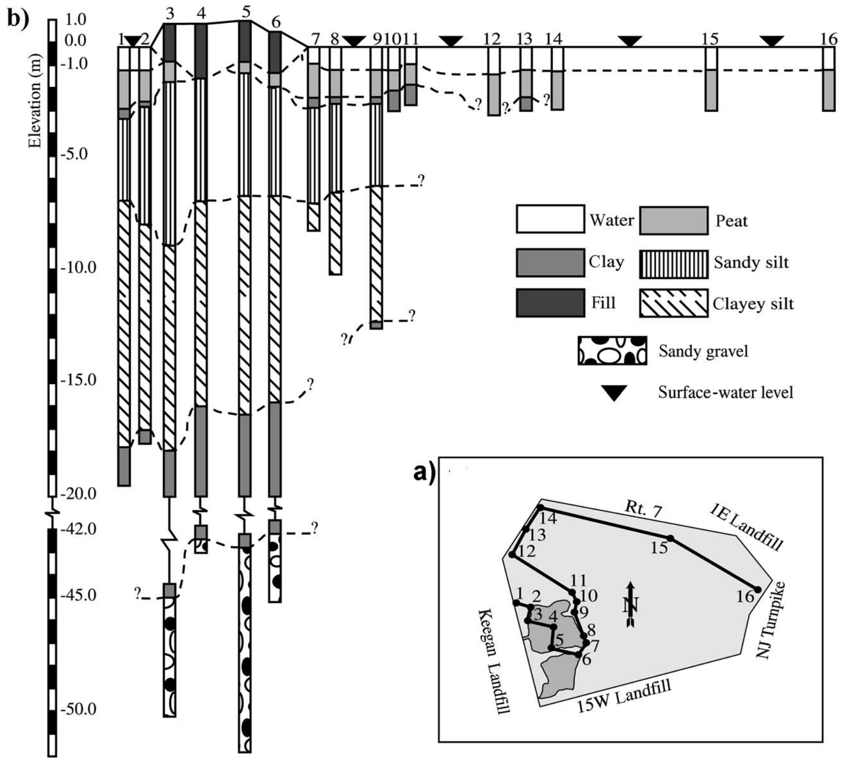

Figure 2. (a) A plan view, showing the locations of boreholes in Kearny Marsh. (b) A cross section showing subsurface stratigraphy and existence, and depth of surface water. The inverted triangles indicate the presence of surface water, the depth of which is shown by the white fill.

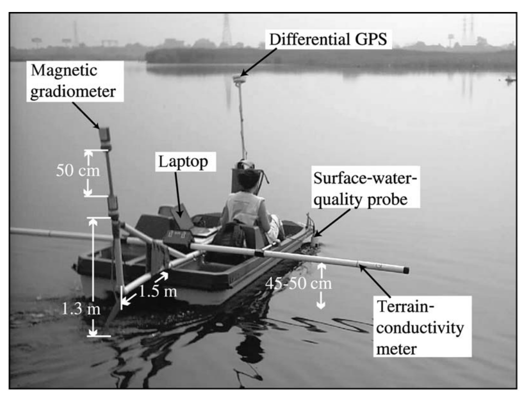

Figure 3. The paddleboat in operation on Kearny Marsh, showing on-board instrumentation. The paddleboat is all-plastic construction except for an aluminum steering mechanism. Annotations show basic survey setup parameters. Note: both the magnetic gradiometer and the terrain-conductivity meter are shown for illustration purposes only; those data were collected on separate surveys to avoid interference among instruments.

SEDIMENT SAMPLING AND LABORATORY ANALYSIS

We also collected 28 bottom-sediment samples to constrain and calibrate the apparent-conductivity measurements recorded in our surveys. Sediment sampling was performed in accordance with the American Society of Testing and Material guidelines (ASTM-D4823), a sampling technique commonly used for unconsolidated, submerged soils. Two sediment samples were obtained from each location using a lake sediment corer equipped with a drop hammer that lacked rotary operation, to minimize disturbance. Samples were collected and sealed directly into plastic liners, thereby requiring no extrusion procedure in the field. Sampling depths ranged between 0 and 60 cm from the top of the marsh sediments. Sampling locations (shown in Figure 1) were selected on the basis of initial results of the EM data and followed a perceived direction of maximum gradient, to investigate trends in the apparent-conductivity data. The following tests were performed: (1) pore-water conductivity; (2) sediment conductivity; and (3) heavy metal analysis, including tests for cadmium, chromium, mercury, nickel, lead, zinc, manganese, and copper (Table 1). Pore water was extracted from the samples by centrifuging and filtering the liquid using a pressure vacuum, and fluid conductivity was measured directly. Sediment conductivity was measured using a four-electrode technique. Sediment samples were subjected to microwave digestion, and heavy metals were measured quantitatively using an atomic absorption spectrometer equipped with a graphite tube atomizer, a programmable sample dispenser, and a vapor-generation accessory for mercury. Quality assurance and quality control for the analytical chemistry were performed dur-

Table 1. Pore-water conductivities and heavy-metal concentrations in the marsh sediments. Locations of the sample sites are shown in Figure 1. [NS: no sediment criterion; LEL: lowest effects limit (based on Ontario aquatic sediment criterion); ND: not detected; SEL: severe effects limit (based on Ontario aquatic sediment criterion); bold: exceeds SEL.].

	Pore-water conductivity values	Bottom-sediment heavy-metal concentrations (mg/kg)								
Sample no.	σ_ω(S/m)	Cd	Cr	Cu	Hg	Mn	Ni	Pb	Zn	Total
1	0.095	2.4	3.2	8.6	0.8	180.7	21.8	35.1	151.9	404.5
2	0.093	7.1	18.2	34.5	**9.3**	212.5	24.9	101.9	640.3	1048.6
3	0.105	1.4	36.6	55.6	0.7	141.4	24.7	125.8	154.0	540.3
4	0.092	4.8	41.5	**112.2**	0.7	180.2	44.6	**326.8**	307.2	1018.1
5	0.151	4.5	2.3	19.3	ND	88.6	21.1	65.0	169.5	370.5
6	0.147	2.8	12.1	36.2	ND	186.9	31.3	90.4	162.9	522.6
7	0.163	5.7	14.3	37.4	ND	142.5	32.9	96.4	316.3	645.5
8	0.158	6.8	**167.3**	**161.8**	1.0	303.2	71.9	**473.1**	588.9	1773.9
9	0.161	1.0	25.1	12.8	0.9	54.3	20.2	33.8	44.8	193.0
10	0.167	3.4	4.1	6.2	0.3	150.1	24.4	45.3	240.7	474.5
11	0.132	4.0	14.3	10.8	ND	221.8	31.0	53.3	484.2	819.4
12	0.124	2.1	7.3	44.0	ND	137.1	25.3	99.3	202.3	517.6
13	0.164	5.0	1.2	8.4	ND	188.4	28.2	64.5	140.0	435.6
14	0.137	2.3	15.1	16.8	1.3	130.4	26.6	55.4	116.8	364.7
15	0.130	0.9	8.1	5.9	ND	95.4	14.0	18.6	158.2	301.0
16	0.154	1.1	4.5	14.5	1.2	79.1	14.9	15.2	85.4	216.0
17	0.173	1.9	14.7	58.0	ND	229.7	33.8	173.5	208.7	720.4
18	0.187	5.2	**155.5**	**215.7**	0.6	553.8	**98.7**	**596.9**	589.5	2215.9
19	0.192	1.7	44.8	**241.8**	0.4	146.6	49.8	**313.9**	225.4	1024.5
20	0.228	**20.0**	38.3	98.5	0.3	281.2	71.7	226.6	221.6	958.3
21	0.202	2.3	9.3	33.3	0.4	129.1	26.2	82.3	178.0	461.0
22	0.208	3.3	35.9	**111.2**	0.3	138.3	48.9	**432.9**	311.0	1081.8
23	0.219	**20.2**	**581.2**	**320.7**	**21.2**	373.8	**123.1**	**617.5**	2422.5	4480.2
24	0.165	3.0	26.9	38.8	0.4	176.9	33.2	136.8	253.1	669.2
25	0.212	5.7	29.4	44.0	ND	159.9	40.9	165.6	248.4	694.1
26	0.241	3.9	**169.8**	**147.7**	ND	233.6	71.2	**448.7**	407.1	1482.1
27	0.165	2.5	20.8	19.1	ND	124.3	28.3	43.4	263.5	501.8
28	0.149	3.1	30.0	11.6	ND	74.8	25.6	51.1	45.4	241.7
Standard deviation		0.7	0.2	0.3	–	7.8	3.6	6.3	1.4	
Relative standard deviation		13.8%	14.0%	4.1%	–	4.2%	12.9%	9.8%	1.0%	
Recovery percentage		102.5%	102.1%	98.7%	99.1%	98.0%	96.5%	100.0%	99.0%	
LEL (mg/kg)		0.6	26.0	16.0	0.2	NS	16.0	31.0	120	
SEL (mg/kg)		10.0	110.0	110.0	2.0	NS	75.0	250.0	820	

ing the analysis by analyzing three duplicate samples, a standard, and blanks.

GEOPHYSICAL DATA PROCESSING

Our survey produced geophysical data sets that had a sampling density of about 12,000 points per 10 km of survey line and generated a total of 33,791 measurements of apparent conductivity and 45,780 measurements of vertical magnetic gradient. As an example of this high density of spatial sampling, Figure 4 shows measurement locations for the terrain-conductivity survey in Kearny Marsh. Data-sampling density was greater around potential pollution sources, such as landfills, metal junkyards, the possible tidal connection to the northeast, and industrial or commercial facilities.

To estimate bottom-sediment resistivities, apparent-conductivity data were inverted using EM1DINV, a one-dimensional laterally constrained inversion (1D-LCI) algorithm originally developed for inverting resistivity data (Auken et al., 2002; Auken and Christiansen, 2004). The forward modeling was done by calculating the vertical magnetic field from a vertical magnetic dipole over a layered half-space (Ward and Hohmann, 1988). The apparent resistivity in the low-frequency approximation, as given by McNeill (1980), is

$$\sigma_a = \frac{4}{\omega\mu_o r^2}\left[\frac{H_s}{H_p}\right] \quad (1)$$

where σ_a is the apparent conductivity, ω is the angular frequency, μ_o is the free-space magnetic permeability, r is the coil separation, H_s is the secondary free-space magnetic field, and H_p is the primary magnetic field. The misfit function used in the 1D-LCI was calculated as the sum of (1) the logarithmic-data misfit normalized by the logarithmic standard deviation of the measured data and (2) the model-parameter misfit normalized by the expected model-parameter standard deviation (Auken and Christiansen, 2004).

The EM31 data set collected at Kearny Marsh was inverted as a two-layer case (water and sediment). The water-layer depth and water-layer resistivity were a priori known parameters that were determined using the surface-water probe. Thus, the only unknown in the inversion was the sediment conductivity of interest. First, the water-layer conductivity values and the EM31 data set were resampled into groups of five data points (the five closest to each other), such that a single model was obtained for each group (the model represented about 20 m^3 of wetland soil). That was done to increase the statistical significance in each inversion result. Those model parameters were tied together laterally with a specified variance factor of 1.1 (as strong lateral constraint), because smooth boundaries were expected in the EM31 data given the fact that the primary control on the sediment conductivity was expected to be contamination-generated variations in pore-fluid conductivity. Generally, the average normalized residual of the inversion was less than 4%, which indicates well-fitted data.

As a final step, inverted conductivities were calibrated to laboratory soil-conductivity measurements performed on the 28 soil samples collected from the site. That was done to compensate for the fact that the EM instrument does not record the true conductivity of the earth. The inverted sediment conductivities at the locations of 28 soil samples collected in the marsh showed a linear relationship with the measured soil conductivity ($\sigma_{soil} = 0.8501\sigma_{inv} + 0.0858$). We attribute the large scatter in this relationship (it had a linear correlation coefficient of 0.25) primarily to the difference in scale between the EM31 measurement (with a support volume of approximately 20 m^3) and the soil-sample measurement (with a support volume of approximately 0.1 m^3). To provide an image of estimated sediment conductivity, the inverted EM data set was dc shifted on the basis of the linear relationship between the inverted sediment conductivity and the measured soil conductivity. A spatial image was created in GIS ArcEditor® 9.0, using standard features such as spatial and 3D analysts. Existing surface-water data and sediment geochemical data and their respective geographic coordinates were converted to database tables and imported into a GIS framework for spatial correlation with geophysical data.

RESULTS AND DISCUSSION

Surface-water data

The surface-water electrical-conductivity (σ_w) measurements we obtained in Kearny Marsh ranged from 0.05 to 0.30 S/m (Figure 5a). Except along the western edge of the marsh, σ_w appears to vary slightly around an average value of 0.25 S/m. Lower σ_w values, ranging from 0.05 to 0.15 S/m, were measured in the western and northwestern parts of the marsh along the metal junkyard and the baseball field, as well as north of the Keegan Landfill (Figure 5a). Around the southern portions of the Keegan Landfill, σ_w increases to values between 0.200 and 0.225 S/m (Figure 5a), and it increases to about 0.25 S/m along the eastern edge of the landfill. The open water in the central and northern parts of the marsh shows consistent, high

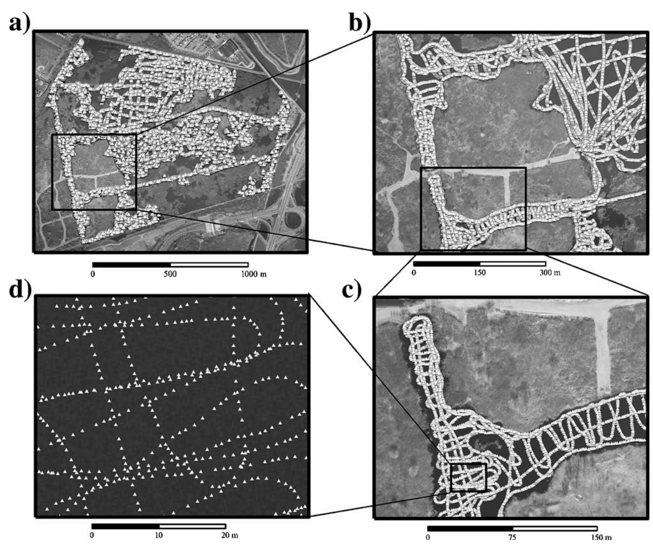

Figure 4. (a) An example of data sampling density of geophysical and surface-water measurements in Kearny Marsh (approximately 80,000 data points). (b) A close-up view around section B of the Keegan Landfill. (c) The southwestern corner of section B. (d) A detailed view, showing average spacing of about 1.5 m in the survey direction.

σ_w values that reach 0.275 S/m. At the eastern side of the marsh, along the New Jersey Turnpike, σ_w ranges from 0.2 to 0.3 S/m.

The surface-water conductivity, imaged in Figure 5a, shows no evidence for a tidal connection in the east-northeast corner of the marsh, as had been suggested previously on the basis of hydrological measurements (Kocis, 1982). Thus, our surface-water measurements support the concept that the marsh became a closed freshwater system following installation of the 1970 extension of the New Jersey Turnpike, which separated Kearny Marsh from the tidal flow of the Hackensack River to the east. Also, our surface-water measurements show no evidence for a surface-water plume associated with the Keegan Landfill.

Surface water in Kearny Marsh generally is alkaline, as indicated by the pH measurements (Figure 5b). Areas around the Keegan Landfill, except at its northern edge, are dominated by high-pH values that range from 9.0 to 9.5. The southern and eastern edges of the marsh are characterized by pH values ranging from neutral to 8.3. The central and northern parts of the marsh are dominated by pH values ranging from 8.0 to 9.0. The lowest pH values (as low as 7.0) are found mostly in the southeast part of the marsh and north of section B of the Keegan Landfill, as well as near the metal junkyard in the northwest. The highest pH values (as high as 9.5) probably reflect the dumping of large amounts of concrete around the Keegan Landfill, wherein dissolved limestone reacts with hydrogen ions and produces carbon dioxide. It is also possible that respiration by algae feeding on nutrients from the landfill generates carbon dioxide, although our surface-water conductivity data (Figure 5a) do not indicate a large increase in nutrient concentration close to the landfill.

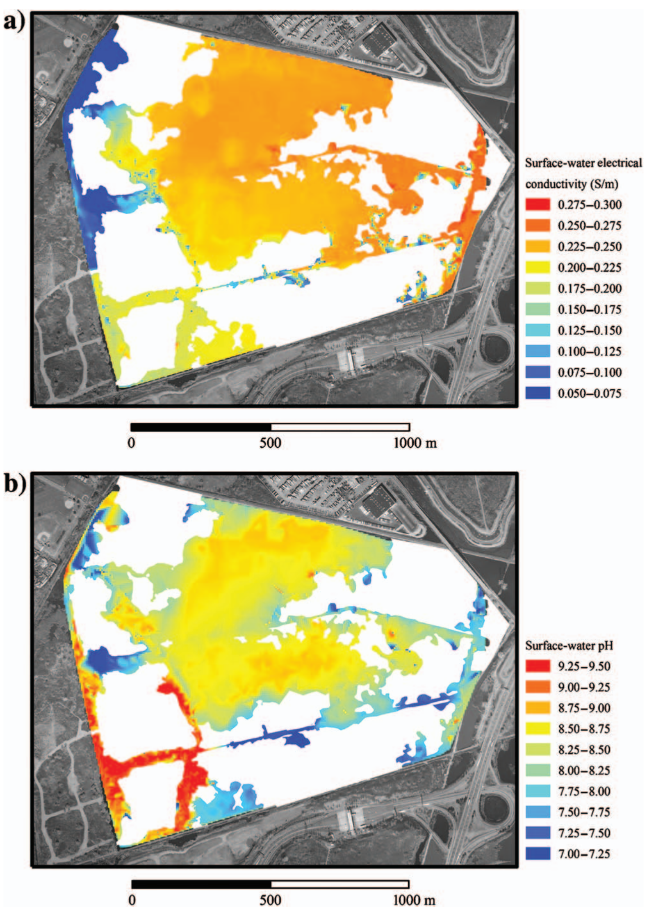

Figure 5. (a) A spatial image showing the distribution of surface-water conductivities (in S/m) in Kearny Marsh. (b) A spatial image showing the distribution of surface-water pH values in Kearny Marsh. In both images, the white shading represents the vegetated areas that defined break lines of the interpolation boundaries.

Sediment conductivity

Apparent-conductivity values are shown in Figure 6a, and the EM1DINV inverted sediment conductivity is imaged in Figure 6b. To facilitate correlations among the apparent-conductivity, inverted sediment-conductivity, and surface-water-conductivity measurements in the marsh, four profile plots are presented in Figure 7 (see Figure 6b for plot locations). Apparent conductivity and inverted sediment conductivity are distributed similarly across the marsh (Figures 6 and 7). Furthermore, spatial distribution of apparent-conductivity values differs distinctly from the σ_w distribution — except

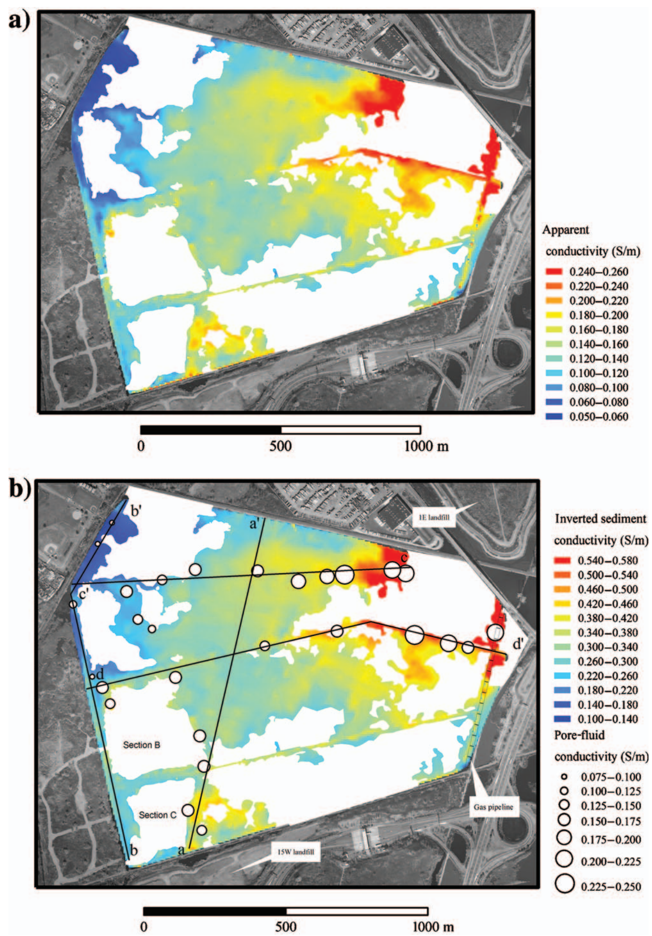

Figure 6. (a) A spatial image, showing the apparent conductivity (in S/m) generated from the high-density geophysical data measurements. (b) A spatial image showing the inverted sediment conductivity (in S/m) generated from inverting and calibrating the raw data using surface water depth, resistivity, height of the EM coils, and direct laboratory soil-conductivity measurements. Pore-water conductivity values (in S/m) from 28 sediment samples are indicated by the varying sizes of the open circles. In both images, the white shading represents the vegetated areas that defined break lines of the interpolation boundaries.

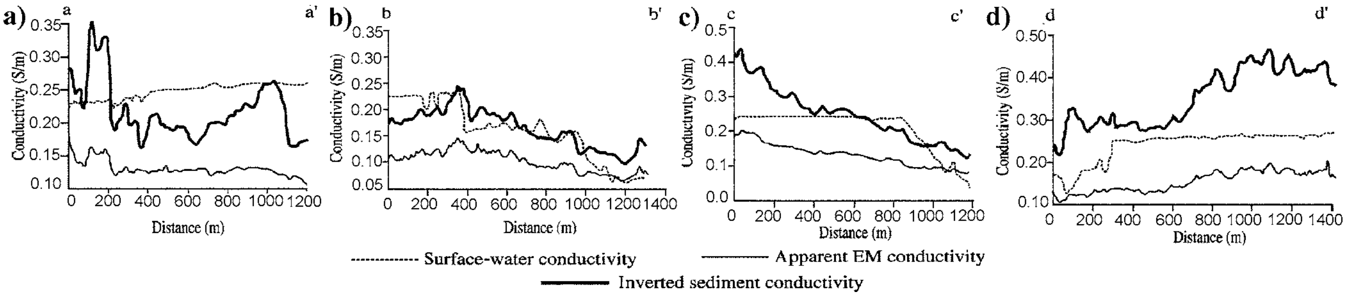

Figure 7. Profiles representing the correlations among surface-water-conductivity measurements, apparent-conductivity values, and true-conductivity measurements of the subsurface generated along: (a) line a-a′ in the north-south direction across the central part of Kearny Marsh, (b) line b-b′ in the north-south direction along the western edge of the marsh, (c) line c-c′ in the east-west direction near the northern part of the marsh, and (d) line d-d′ in the east-west direction across the middle of the marsh.

along the western edge, where σ_w correlates with the apparent conductivity and the inverted sediment conductivity, as shown along line b-b′ (Figure 7). However, Figure 7 clearly demonstrates the important finding that the apparent-conductivity measurement is sensitive primarily to the sediment-conductivity values (the parameter of interest) in this shallow-water wetland.

Inverted sediment-conductivity values range from 0.10 to 0.58 S/m and show a general increase toward the east-northeast (Figures 6b and 7). The lowest inverted sediment conductivities, ranging from 0.10 to 0.35 S/m, occur in the western and northwestern parts of the marsh, alongside the metal junkyard and the baseball field (Figure 7b). The central and northern parts of the marsh are dominated by moderate sediment-conductivity values that range from 0.20 to 0.46 S/m, whereas the northeastern corner of the marsh shows higher values of inverted sediment conductivity that reach 0.58 S/m (Figures 6b, 7c, and d). The areas around the Keegan Landfill show two trends: low to moderate inverted sediment-conductivity values, ranging from 0.10 to 0.25 S/m, dominate the western parts (Figure 7b), whereas significantly higher conductivity values, reaching as high as 0.35 S/m, dominate the eastern parts of the Keegan Landfill (Figure 8a).

The region of highest sediment conductivity, mapped in the northeastern corner of Kearny Marsh, may indicate (1) a groundwater plume emanating from the 1E Landfill, (2) lithologic change, with electrically conductive sediments existing toward the northeast, or (3) residual higher salinity values in the sediments closest to the point at which a tidal connection existed before 1970 (Figure 1). Available lithologic data do not indicate any significant lithologic change in the upper 3 m of sediment (see the traverse from cores 14 through 16 in Figure 2). Pore-water conductivities measured from samples collected close to the metal junkyard and the baseball field are between 0.075 and 0.125 S/m, whereas sediment samples collected from the northeastern corner of the marsh close to the 1E Landfill exhibit the highest pore-water conductivities, which range between 0.200 and 0.250 S/m (Figure 6b). Furthermore, heavy metal concentrations generally are highest in the northeastern corner of the marsh (Table 1, Figure 1). Thus, we believe that the high values of inverted sediment conductivity in the northeastern part of the marsh result from increases in pore-water conductivity and that those increases stem from contamination either by landfill leachates or by salts associated with the old tidal connection. The inverted sediment-conductivity image also indicates a possible groundwater plume flowing from Section C of the Keegan Landfill and/or the 15W Landfill toward the south (Figure 6b). Pore-water samples collected around the Keegan Landfill have conductivities ranging from 0.125 S/m to the west of the landfill to about 0.175 S/m to the east. Heavy-metal concentrations also are higher east of the landfill, relative to concentrations at its western edge.

This analysis suggests that the use of a 1D-LCI, when constrained by depth and resistivity measurements of the surface-water layer as a priori known parameters, is an effective method for imaging the pattern of sediment conductivity across a wetland. Parameter-sensitivity analysis showed that the inverted sediment conductivity was determined with an uncertainty of less than 4%. These well-resolved

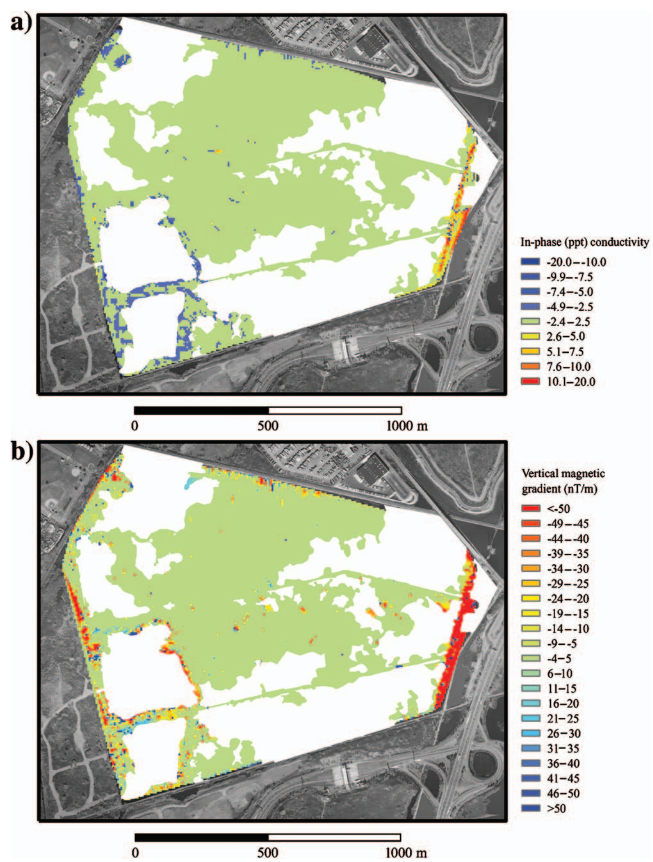

Figure 8. Spatial images showing (a) the in-phase measurements of the EM31 data (in ppt) generated from the high-density geophysical data measurements, and (b) magnetic gradiometer values (in nT/m) generated from the high-density geophysical data measurements. In both images, the white shading represents the vegetated areas in Kearny Marsh.

parameters result from the facts that (1) surface-water conductivity and surface-water depth were fully constrained with the continuous data obtained from the surface-water probe, and (2) water depths are shallow in this application. Although the range of apparent-conductivity values (0.05–0.30 S/m) extends slightly into the region in which the EM31 quadrature response begins to deviate from its linearity with the true subsurface conductivity (at 0.1 S/m) (McNeill, 1980), that overlap is accounted for in the inversion process because the forward code calculates the apparent conductivity in the same way that the instrument measures it (i.e., from equation 1). Consequently, the anomalously high conductivity regions in the marsh, notably those around the 1E Landfill, probably are more conductive than estimated from the 1D-LCI.

Magnetic-gradiometer and in-phase data

Figure 8a presents in-phase measurements of terrain conductivity, whereas Figure 8b presents the vertical magnetic-gradiometer values. In-phase conductivity is characterized by low values (ranging only to ±2.5 ppt) across the marsh, but we see localized high values (as high as ±20 ppt) around the Keegan Landfill, along the eastern and the northern edges of the marsh, and along the baseball field and the metal junkyard to the west and northwest (Figure 8a). The magnetic-gradiometry image is characterized by high anomalies (exceeding ±50 nT/m) superimposed on a background magnetic gradient of ±10 nT/m (Figure 8b). The anomalies of the in-phase data and the vertical magnetic gradient generally agree, thereby indicating that buried ferromagnetic and metallic debris is scattered extensively throughout the marsh but is concentrated around the Keegan Landfill. The linear anomaly along the eastern edge of the marsh is the response to a buried gas-utility line. Localized anomalies near the center of the marsh result from a partially submerged abandoned vehicle (SUV) and several automobile wheels visually recorded during the survey.

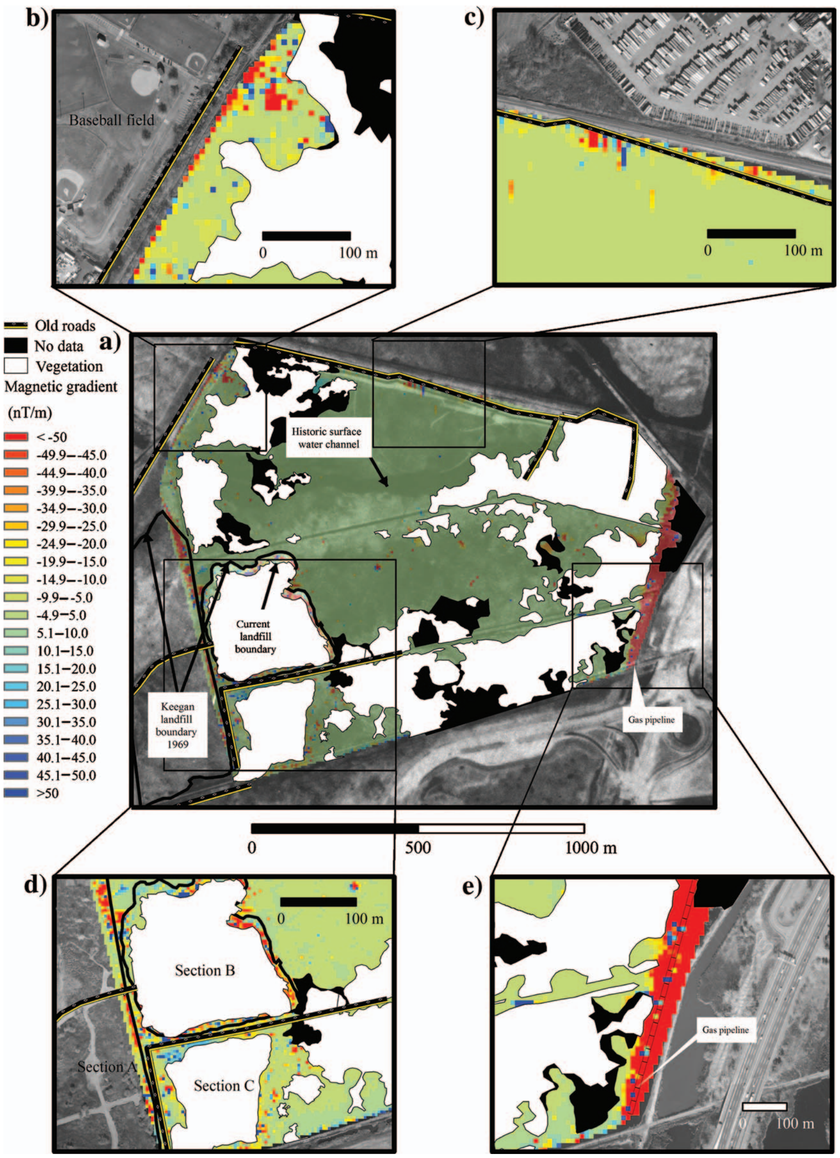

Figure 9. (a) A multilayer spatial image showing an aerial view of Kearny Marsh in 1969, with the extent of the Keegan Landfill and the trends of old roads outlined, and a magnetic-gradiometry image with 65% transparency. The white shading represents present dry and vegetated areas within Kearny Marsh. The historic surface-water channel is shown trending east to west and is limited to the central part of the marsh. (b) A close-up of the area east of the baseball field, showing the magnetic anomalies where most current littering exists. (c) The trend of a historic old road in the northern part of the marsh, coinciding with a magnetic anomaly. (d) The maximum extent of the Keegan Landfill, outlined from the 1969 aerial photos, and the trend of the magnetic anomaly. (e) The southeastern corner of the marsh, showing the location of the buried gas pipeline and the magnetic anomaly.

We attribute the distribution of buried ferromagnetic and metallic debris in the marsh, as mapped with vertical gradiometry data and the in-phase component of the EM31 data, to a legacy of land misuse and environmental degradation. Most of the anomalies in the marsh were detected by both the in-phase and the vertical-gradiometer measurements (Figure 8). Although both the in-phase and vertical-gradiometer measurements agree closely, the magnetic gradiometer provided higher spatial resolution of the ferromagnetic junk metal. Furthermore, certain places exhibit anomalies recorded by the in-phase component only, which may be attributed to debris that is nonferromagnetic but is electrically conductive.

Aerial photographs from 1969, when the Keegan Landfill was operational, support this theory of a legacy of land misuse and environmental degradation. The 1969 aerial photographs were precisely rectified and spatially registered to overlie the geophysical data sets (Figure 9). The old boundary of the Keegan Landfill and old access roads were identified and outlined. Note that no water divide existed between section A and sections B and C of the Keegan Landfill at that time. In fact, surface water was limited to a channel located in the central portion of the marsh (Figure 9a). This overlay image shows that debris is present primarily in four parts of the marsh. These locations are: (1) around sections B and C of the Keegan Landfill (Figure 9d), (2) within a circular area adjacent to the baseball field (Figure 9b), (3) along the eastern boundary of the marsh adjacent to the New Jersey Turnpike (Figure 9e), and (4) along Belleville Turnpike north of the marsh (Figure 9c).

Figure 9 shows that the magnetic-gradiometer data appear to map the maximum operational extent of the Keegan Landfill. Water levels in Kearny Marsh have increased since 1969, eventually covering the edges of the Keegan Landfill and changing its morphology. Section B of the Keegan Landfill currently is smaller than its 1969 boundary, which extended about 25 to 30 m into the current open water (Figure 9). Furthermore, the gradiometer anomalies mapped near the Belleville Turnpike and along the southern parts of the Keegan Landfill align with access roads that existed in 1969. The gradiometer data therefore appear to reflect historical dumping associated with those access roads. Illegal dumping also is associated with marshland immediately proximal to the metal junkyard and the baseball field.

CONCLUSIONS

We have shown that surveys from a paddleboat equipped with geophysical sensors, surface-water sensors, and a precision GPS instrument provide an effective approach for reconnaissance characterization of wetlands. Paddleboat surveys have two advantages: (1) the boat's shallow draft permits rapid data acquisition in less than 1 m of water, where conventional direct-water sampling and sediment sampling is difficult, and (2) geophysical sensors are housed without detectable interference from the vessel.

The apparent and inverted sediment conductivities correlate well and parameter uncertainties are low in sediment-conductivity values obtained from a laterally constrained inversion. The inversion of terrain conductivity results in images of sediment conductivity that, in our case study, indicate the distribution of elevated pore-water conductivity in the marsh sediments. That distribution of elevated pore-water conductivity probably reflects either leachates emanating from landfills peripheral to the marsh or the residual effect of a past tidal connection. In-phase and gradiometer data define the distribution of ferromagnetic and metallic debris and reveal a legacy of illegal dumping, which is supported by historical land-use data. We propose that noninvasive geophysical imaging provides a new way to study shallow-water-wetland environments.

ACKNOWLEDGMENTS

This project was supported by a grant from the United States Department of Interior — Geological Survey through the New Jersey Water Resources Research Institute (NJWRRI) and a grant from the Meadowlands Environmental Research Institute (MERI). The authors thank former MERI research director Kirk Barrett and former MERI director Nabil Adam for supporting this project. Dom Elfante (MERI) assisted with the GIS component of this work. Rutgers students Tammy Trubacco, Malik Jang Baz, and Rachel Price assisted with fieldwork.

REFERENCES

Auken, E., and A. V. Christiansen, 2004, Layered and laterally constrained 2D inversion of resistivity data: Geophysics, **69**, 752–761.

Auken, E., N. Foged, and K. I. Sørensen, 2002, Model recognition by 1D laterally constrained inversion of resistivity data: 9th meeting, Environmental and Engineering Geophysical Society, European Section, 241–244.

Benson, A. K., K. L. Payne, and M. A. Stubben, 1997, Mapping groundwater contamination using DC resistivity and VLF geophysical methods — A case study: Geophysics, **62**, 80–86.

Buselli, G., and K. Lu, 2001, Groundwater contamination monitoring with multichannel electrical and electromagnetic methods: Journal of Applied Geophysics, **48**, 11–23.

Furness, P., 2002, The magnetic field of steel drums: Journal of Applied Geophysics, **51**, 63–74.

Greenhouse, J., and R. Harris, 1983, Migration of contaminants in groundwater at a landfill: A case study: 7. DC, VLF, and inductive resistivity surveys: Journal of Hydrology, **63**, 177–197.

Kachanoski, R. G., E. G. Gregorich, and I. J. Van Wesenbeeck, 1988, Estimating spatial variations of soil water content using non-contacting electromagnetic inductive methods: Canadian Journal of Soil Science, **68**, 715–722.

Kobr, M., and I. Linhart, 1994, Geophysical survey as a basis for regeneration of waste dump Halde 10, Zwickau, Saxony: Journal of Applied Geophysics, **31**, 107–116.

Kocis, J. M., 1982, The Kearny freshwater marsh: The dynamics of a young freshwater marsh: Hackensack Meadowlands Development Commission (HMDQ) Basin Management Plans, 29.

Langan Engineering and Environmental Services (LEES), 1999, Sediment and water sampling report, Kearny Marsh, New Jersey.

Matias, M. S., M. M. da Silva, P. Ferreira, and E. Ramalho, 1994, A geophysical and hydrogeological study of aquifers contamination by a landfill: Journal of Applied Geophysics, **31**, 155–162.

McNeill, J. D., 1980, Electromagnetic terrain conductivity measurements at low induction numbers: Geonics Limited: Technical Note TN-6.

———, 1990, Use of electromagnetic methods for groundwater studies, *in* S. N. Ward, ed., Geotechnical and environmental geophysics, 1: Review and Tutorial: SEG, 191–218.

Meju, M. A., 2000, Geoelectrical investigation of old/abandoned, covered landfill sites in urban areas: Model development with a genetic diagnosis approach: Journal of Applied Geophysics, **44**, 115–150.

Pozza, M. R., J. I. Boyce, and W. A. Morris, 2004, Lake-based magnetic mapping of contaminated sediment distribution, Hamilton Harbor, Lake Ontario, Canada: Journal of Applied Geophysics, **57**, 23–41.

Ravat, D., 1996, Magnetic properties of unrusted steel drums from laboratory and field magnetic measurements: Geophysics, **61**, 1325–1335.

Roberts, R. L., W. J. Hinze, and D. I. Leap, 1990, Data enhancement procedure on magnetic data from landfill investigations, *in* S. H. Ward, ed., Geotechnical and environmental geophysics, 2: Environmental and groundwater: SEG, 261–266.

Sheets, K. R., and J. M. H. Hendrickx, 1995, Noninvasive soil water content measurement using electromagnetic induction: Water Resources Research, **31**, 2401–2409.

Smith, R. D., A. Ammann, C. Bartoldus, and M. M. Brinson, 1995, An approach for assessing wetland functions using hydrogeomorphic classification, reference wetlands, and functional indices: Vicksburg, Mississippi, U. S. Army Corps of Engineers, Waterways Experiment Station, Technical Report TRWRP-DE 10, 100.

Uranowski, C., Z. Lin, M. DelCharco, C. Huegel, J. Garcia, I. Bartsch, M. Flannery, S. Miller, J. Bacheler, and W. Ainslie, 2003, A Regional guidebook for applying the hydrogeomorphic approach to assessing wetland functions of low-gradient, blackwater riverine wetlands in peninsular Florida, ERDC/EL TR-03-3, U. S. Army Corps of Engineers, Engineer Research and Development Center.

Ward, S. H., and G. W. Hohmann, 1988, Electromagnetic theory for geophysical applications, *in* M. N. Nabighian, ed., Electromagnetic methods in applied geophysics, 1: SEG, 131–308.

Woldt, W. E., M. E. Hagemeister, and D. D. Jones, 1998, Characterization of an unregulated landfill using surface-based geophysics and geostatistics: Ground Water, **36**, 966–974.